Thermophysical properties of liquid UO_2, ZrO_2 and corium by molecular dynamics and predictive models

Woong Kee Kim[a], Ji Hoon Shim[a,c,*] and Massoud Kaviany[a,b,*]

[a]*Division of Advanced Nuclear Engineering, Pohang University of Science and Technology, Pohang 37673, Korea*
[b]*Department of Mechanical Engineering, University of Michigan, Ann Arbor, Michigan 48109-2125, USA*
[c]*Department of Chemistry, Pohang University of Science and Technology, Pohang 37673, Korea*
[*]*Corresponding author: : kaviany@umich.edu*

1. Introduction

In severe accident of light-water reactors, lava-like molten mixture called corium (compounds of UO_2, ZrO_2 and Zr) is created due to the radioactive decay and heat of fission. The analysis of such accidents (fate of the melt), requires accurate corium thermophysical properties data up to 5000 K [1]. In addition, the initial corium melt superheat melt, determined from such properties, are key in predicting the fuel-coolant interactions (FCIs) [2] and convection and retention of corium in accident scenarios, e.g., core-melt down corium discharge from reactor pressure vessels and spreading in external core-catcher [3,4]. Due to the high temperatures, data on molten corium and its constituents are limited, so there are much data scatters and mostly extrapolations (even from solid state) have been used [5]. Here we predict the thermophysical properties of molten UO_2 and ZrO_2 using classical molecular dynamics (MD) simulations (properties of corium are predicted using the mixture theories and UO_2 and ZrO_2 properties). The empirical interatomic potential models are critical in accurate MD prediction of the properties, and the molten corium constituent oxides, especially UO_2, have several models developed for the solid phase(s), each tuned to different bulk properties. We compare the predictions and decipher the differences, compare with theoretical predictive models for these properties, and select the most relevant of these models. The predicted properties are density, heat capacity, compressibility, viscosity, thermal conductivity and surface tension up to 5000 K and their temperature-dependent useful correlations are provided.

2. Methods and Results

2.1 Interatomic potential models for UO2 and ZrO2

We used the LAMMPS [6] package for the MD simulations to predict liquid corium properties from atomistic approach. Liquid corium has no microstructure, so microscopic properties can be the same as the measured macroscopic (bulk) ones. For predicting low symmetry (e.g., liquids) systems efficiently [7] the interatomic potential models have evolved, e.g., reactive force field [8] and 2NN MEAM [9] formalism. To describe the overlap of the atomic orbitals, the embedded-atom method (EAM) [10] for UO_2 and ZrO_2 is proposed by Cooper et al. (CRG) [11,12], while the traditional Buckingham model [13] for ZrO_2 is introduced by De *et al*. (Teter) [14]. The CRG models additionally consider the many-body perturbations to the Buckingham-Morse potentials. It models the coordinate-dependent bonding and violation of the Cauchy relation [15] by the many-body perturbations. The energy of atom i surrounded by atom j is

$$\varphi_i=\frac{1}{2}\sum_j \phi_{\alpha\beta}(r_{ij}) - G_\alpha \left[\sum_j \sigma_\beta(r_{ij})\right]^{\frac{1}{2}}, \quad (1)$$

where α and β are elements of atoms i and j. In Eq. (1), The first term combines the short-range pairwise interaction using the Buckingham [13] and Morse [16] potentials an the long-range electrostatic Coulomb interactions, i.e.,

$$\phi_{\alpha\beta}(r_{ij})=A_{\alpha\beta}\exp\left(-\frac{r_{ij}}{\rho_{\alpha\beta}}\right) - \frac{C_{\alpha\beta}}{r_{ij}^6} + D_{\alpha\beta}\left\{\exp\left[-2\gamma_{\alpha\beta}(r_{ij}-r_o)\right] - 2\exp\left[-\gamma_{\alpha\beta}(r_{ij}-r_o)\right]\right\} + \frac{q_\alpha q_\beta}{4\pi\epsilon_0 r_{ij}}. \quad (2)$$

The parameters for the short-range pairwise terms and the ionic charges of the Coulombic terns are listed in Table 1.

	U-U	Zr-Zr	U-O	Zr-O	O-O
$A_{\alpha\beta}$ (eV)	18600	18600	448.779	1147.471	830.283
$\rho_{\alpha\beta}$ (Å)	0.2747	0.23066	0.387758	0.32235	0.352856
$C_{\alpha\beta}$ (eVÅ^6)	0.0	0.0	0.0	0.0	3.884372
$D_{\alpha\beta}$ (eV)	-	-	0.66080	1.2269	-
$\gamma_{\alpha\beta}$ (Å)	-	-	2.05815	1.4482	-
r_o (Å^{-1})	-	-	2.38051	1.998	-
q_U (e)	+2.2208				
q_{Zr} (e)	+2.2208				

q_O (e)	-1.1104

The second term is a subtle many-body perturbation from the surrounding ions in the EAM formalism and was originally expressed as an approximate function of the electron density functional theory (DFT) for metals [17], with a mathematical analogy to the ionic systems [18], and is

$$\sigma_\beta(r_{ij}) = \left(\frac{n_\beta}{r_{ij}^{\delta}}\right)\frac{1}{2}\{1+\mathrm{erf}[20(r_{ij}-1.5)]\}, \quad (3)$$

where G_α is embedding function or energy and σ_β is a set of pairwise functions. The error function prevents unrealistic dynamics when atoms are very close. The parameters for this many-body terms are listed in Table 2.

Table 2. Parameters of the many-body interactions in the CRG models [11,12].

	U	Zr	O
G_α (eV Å$^{1.5}$)	1.806	1.597	3450.995
n_β (Å^5)	0.690	1188.786	106.856

The Teter potential describes the interaction for ZrO_2 using the short-range Buckingham potential model with the long-range Coulombic interaction.

$$\phi_{\alpha\beta}(r_{ij}) = A_{\alpha\beta}\exp\left(-\frac{r_{ij}}{\rho_{\alpha\beta}}\right) - \frac{C_{\alpha\beta}}{r_{ij}^{6}} + \frac{q_\alpha q_\beta}{4\pi\epsilon_0 r_{ij}} \quad (4)$$

	Zr-O	O-O
$A_{\alpha\beta}$ (eV)	7747.1834	2029.2204
$\rho_{\alpha\beta}$ (Å)	0.252623	0.343645
$C_{\alpha\beta}$ (eVÅ^6)	93.109	192.58
q_U (e)	+2.4	
q_O (e)	-1.2	

Table 3. Parameters of the Buckingham potentials for the Teter model [14], and related ionic charges in the Coulombic interactions.

2.2 Melting procedure

The UO_2 and ZrO_2 systems are fluorite crystals and are first melted at very high temperatures (around 5000 K) under the *NPT* ensemble for 20 ps with periodic boundary conditions (PBC) and 12000 atoms. The Nose-Hoover thermostat [25,26] and the Parrinello-Rahman barostat [27] are used for controlling temperature and pressure. The liquid state is verified from the atomic structure, trajectories of atoms and the radial distribution function (RDF). Figure 1 show snapshots using OVITO [28] and radial distribution functions for liquid UO_2 and ZrO_2 at 4000 K.

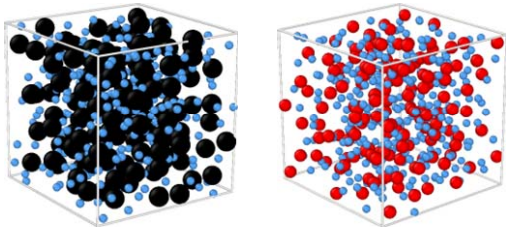

Fig.1. Atomic structures for liquid (a) UO_2 (left) and ZrO_2 (right) at 4000K, showing liquid state. Black, red and blue spheres denote U, Zr and O atoms.

2.3 Density

Densities of liquid UO_2 (black squares) and ZrO_2 (red squares) depending on are predicted by MD simulations using the CRG potential model (Fig. 6). Temperature range of prediction is from near the melting point (3200 K for UO_2 and 3000K for ZrO_2) to 5000 K.

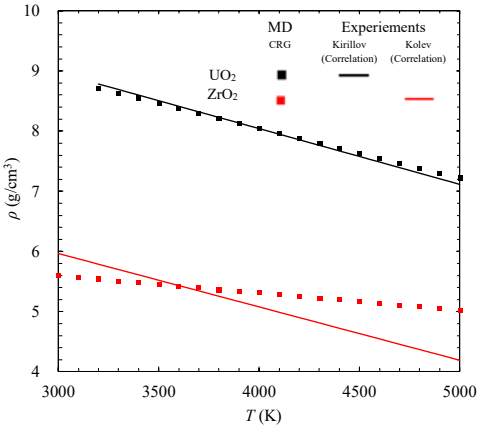

Fig. 2. Variations of MD predicted liquid UO2 and ZrO2 density with temperature, using the CRG potential model and comparison with experiments

2.4 Heat capacity

Heat capacity of liquid UO_2 and ZrO_2 are predicted. In MD simulations, heat capacity is attained from total energy slope, which can be calculated with increasing system temperature up to 5000K. Predicted heat capacities are compared with reported experimental result for both UO_2 and ZrO_2. Heat capacity for ZrO_2 is proposed to 815 J/kg-K as the constant.

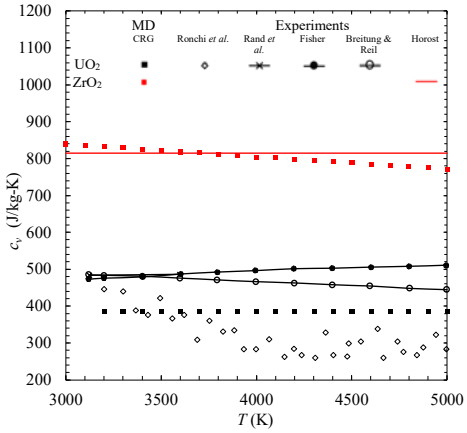

Fig. 3. Variations of MD predicted of liquid UO2 and ZrO2 specific heat at constant volume with temperature, and comparison with experimental results.

2.5 Isothermal compressibility

Isothermal compressibility of liquid UO_2 and ZrO_2 are predicted by equilibrium MD simulations using the CRG and the Teter potentials. In the MD simulations, isothermal compressibility is attained from the volume fluctuation under NPT ensemble, i.e.,

$$\left\langle \delta V^2 \right\rangle_{\mathrm{NPT}} = \kappa V k_{\mathrm{B}} T \,, \quad (5)$$

where κ,V, k_{B} and T are compressibility, volume of the system, Boltzman constant and temperature respectively. $< >$ denotes averaging value with time.

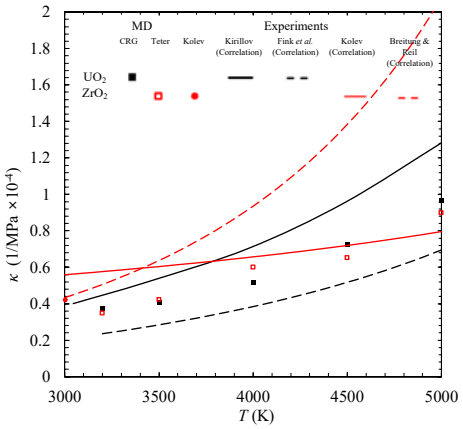

Fig. 4. Variations of MD predicted liquid ZrO_2 compressibility with temperature, using two different sets of interatomic potential models, and comparison with experiments.

2.6 Viscosity

Based on Green-Kubo formula explained in section 4.1.1, viscosity of liquid UO_2 (black squares) and ZrO_2 (red squares) are predicted by MD simulations (see Fig. 5.). Size effect is checked negligible in overall systems on applying Green-Kubo formula for viscosity. Predicted viscosities are compared to reported experimental result and predictive Andrade model (solid lines). Andrade models shows good agreement with MD simulation results for both UO_2 and ZrO_2.

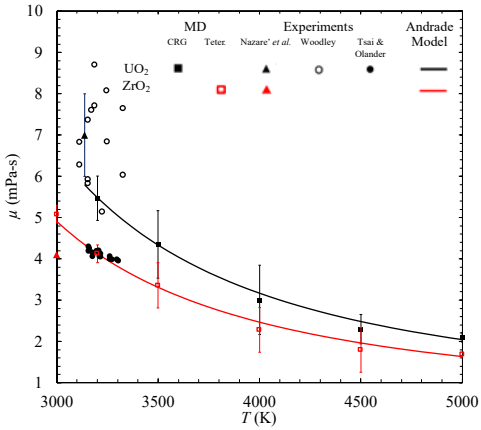

Fig. 5. Variations of MD predicted liquid UO_2 and ZrO_2 viscosity with temperature, and comparison with experiments and with predictive model.

Figure 6 shows viscosity of liquid UO_2-ZrO_2 mixture (corium) depending on temperature and compositions. Blending equation is applied for Andrade models for UO_2 and ZrO_2

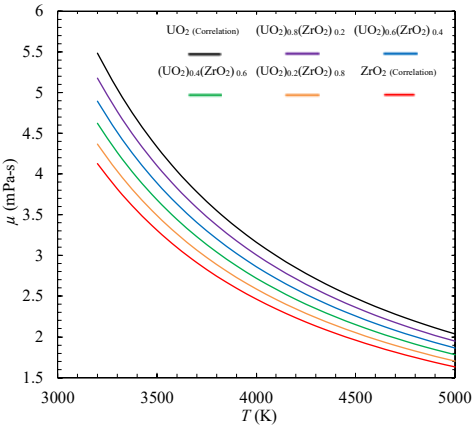

Fig. 6. Variations of liquid UO_2-ZrO_2 mixture (corium) viscosity with temperature, and for several compositions

2.7 Surface tension

Surface tension of liquid UO_2 is predicted by MD simulation. Surface tension is obtained using methodology explained in Eq. (32) in section 5.1. Temperature dependence of surface tension by MD simulations (black squares) is shown in Fig. 18 with experiments (black solid line). Predicted UO_2 surface tension have nearly same values and trends with experimental relation.

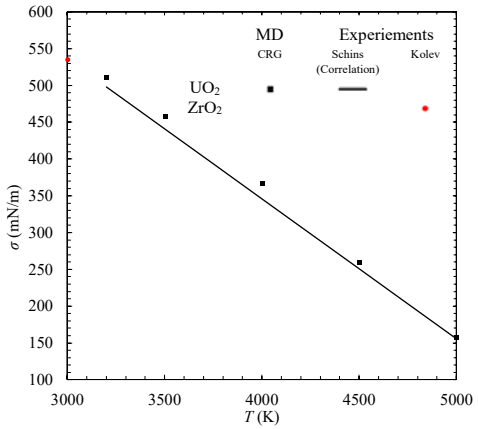

Fig. 6. Variations of MD predicted liquid UO_2 surface tension with temperature, and comparison with experiments (UO_2 and ZrO_2).

3. Conclusions

The thermophysical properties (density, compressibility, heat capacity, viscosity and surface tension) of liquid UO_2 and ZrO_2 are predicted using classical molecular dynamics simulations, up to 5000 K. For atomic interactions, the CRG and the Teter potential models are found most appropriate. The liquid behavior is verified with the random motion of the constituent atoms and the pair-distribution functions, starting with the solid phase and raising the temperature to realize liquid phase. The viscosity and thermal conductivity are calculated with the Green-Kubo autocorrelation decay formulae and compared with the predictive models of Andrade and Bridgman. For liquid UO_2, the CRG model gives satisfactory MD predictions. For ZrO_2, the density is reliably predicted with the CRG potential model, while the compressibility and viscosity are more accurately predicted by the Teter model. The surface tension for UO_2 is reasonably predicted compared to experimental results, whereas the predicted ZrO_2 results by the CRG and the Teter models do not appear reasonable. Newly proposed temperature–dependent correlations for liquid UO_2 and ZrO_2 and corium density, compressibility, heat capacity, viscosity, surface tension, and thermal conductivity are provided in Table 5.

REFERENCES

[1]P. Piluso, J. Monerris, C. Journeau, G. Cognet, Viscosity Measurements of Ceramic Oxides by Aerodynamic Levitation, Int. J. Thermophys. 23 (2002) 1229–1240. doi:10.1023/A:1019844304593.

[2]G. Hwang, M. Kaviany, K. Moriyama, H.S. Park, B. Hwang, Ex-vessel Corium-melt Cooling in Water Pool : Roles of Melt Superheat and Sintering in Sediment, n.d.

[3]D.A. Macinnes, D. Martin, A CALCULATION OF THE ELECTRON BAND GAP IN MOLTEN UO2, J. Nucl. Mater. 98. 98 (1981) 241–246.

[4]S.S. Abalin, V.G. Asmolov, V.D. Daragan, E.K. D'yakov, A.V. Merzlyakov, V.Y. Vishnevsky, Corium kinematic viscosity measurement, Nucl. Eng. Des. 200 (2000) 107–115. doi:10.1016/S0029-5493(00)00238-7.

[5]D.A. MacInnes, D. Martin, A calculation of the electron band gap in molten UO2, J. Nucl. Mater. 98 (1981) 241–246. doi:10.1016/0022-3115(81)90150-1.

[6 S. Plimpton, Fast Parallel Algorithms for Short-Range Molecular Dynamics, J. Comput. Phys. 117 (1995) 1–19. doi:10.1006/jcph.1995.1039.

[7]V. Levitin, The Tight-Binding Model and Embedded-Atom Potentials, in: Interat. Bond. Solids, Wiley-VCH Verlag GmbH & Co. KGaA, New York, NY, 2013: pp. 157–174. doi:10.1002/9783527671557.ch11.

[8 A.C.T. van Duin, S. Dasgupta, F. Lorant, W.A. Goddard, ReaxFF: A Reactive Force Field for Hydrocarbons, J. Phys. Chem. A. 105 (2001) 9396–9409. doi:10.1021/jp004368u.

[9]B.-J. Lee, M.I. Baskes, Second nearest-neighbor modified embedded-atom-method potential, Phys. Rev. B. 62 (2000) 8564.

[10]M.S. Daw, S.M. Foiles, M.I. Baskes, The embedded-atom method: a review of theory and applications, Mater. Sci. Reports. 9 (1993) 251–310. doi:10.1016/0920-2307(93)90001-U.

[11]M.W.D. Cooper, M.J.D. Rushton, R.W. Grimes, A many-body potential approach to modelling the thermomechanical properties of actinide oxides., J. Phys. Condens. Matter. 26 (2014) 105401. doi:10.1088/0953-8984/26/10/105401.

[12]X.-Y. Liu, M.W.D. Cooper, K.J. Mcclellan, J.C. Lashley, D.D. Byler, C.R. Stanek, et al., Thermal transport in UO2 with defects and fission products by molecular dynamics simulations, Los Alamos National Laboratory (LANL), 2015.

[13]R.A. Buckingham, The Classical Equation of State of Gaseous Helium, Neon and Argon, Proc. R. Soc. London A Math. Phys. Eng. Sci. 168 (1938) 264–283. http://rspa.royalsocietypublishing.org/content/168/933/264.abstract.

[14]J. Du, R. Devanathan, L. Corrales, W. Weber, A. Cormack, Short- and medium-range structure of amorphous zircon from molecular dynamics simulations, Phys. Rev. B. 74 (2006) 214204. doi:10.1103/PhysRevB.74.214204.

[15]C.-S. Zha, H. Mao, R.J. Hemley, Elasticity of MgO and a primary pressure scale to 55 GPa, Proc. Natl. Acad. Sci. 97 (2000) 13494–13499. doi:10.1073/pnas.240466697.

[16]P.M. Morse, Diatomic Molecules According to the Wave Mechanics. II. Vibrational Levels, Phys. Rev. 34 (1929) 57–64. doi:10.1103/PhysRev.34.57.

[17]G.J. Ackland, Comprehensive Nuclear Materials, in: Compr. Nucl. Mater., Elsevier, Amsterdam, AE, 2012: pp. 267–291. doi:10.1016/B978-0-08-056033-5.00026-4.

[18]W.K. Kim, J.H. Shim, M. Kaviany, UO2 bicrystal phonon grain-boundary resistance by molecular dynamics and predictive models, Int. J. Heat Mass Transf. 100 (2016) 243–249. doi:10.1016/j.ijheatmasstransfer.2016.04.071.

[19]J.J.P. Stewart, Mopac2009, stewart computational chemistry, colorado springs, co, usa, Web:''http://OpenMOPACnet. (2008).

[20]D. Wolf, Reconstruction of NaCl surfaces from a dipolar solution to the Madelung problem, Phys. Rev. Lett. 68 (1992) 3315–3318. doi:10.1103/PhysRevLett.68.3315.

[21]D. Wolf, P. Keblinski, S.R. Phillpot, J. Eggebrecht, Exact method for the simulation of Coulombic systems by

spherically truncated, pairwise r(-1) summation, J. Chem. Phys. 110 (1999) 8254–8282. doi:10.1063/1.478738.
[22]P.P. Ewald, Die Berechnung optischer und elektrostatischer Gitterpotentiale, Ann. Phys. 369 (1921) 253–287. doi:10.1002/andp.19213690304.
[23]R.W. Hockney, J.W. Eastwood, Computer Simulation Using Particles; Adam Hilger: New York, 1989, There Is No Corresp. Rec. This Ref. (n.d.).
[24]E.L. Pollock, J. Glosli, Comments on P3M, FMM, and the Ewald method for large periodic Coulombic systems, Comput. Phys. Commun. 95 (1996) 93–110. doi:10.1016/0010-4655(96)00043-4.
[25]W.G. Hoover, Canonical dynamics: Equilibrium phase-space distributions, Phys. Rev. A. 31 (1985) 1695–1697. http://link.aps.org/doi/10.1103/PhysRevA.31.1695.
[26]S. Nosé, A unified formulation of the constant temperature molecular dynamics methods, J. Chem. Phys. 81 (1984).
[27]M. Parrinello, A. Rahman, Polymorphic transitions in single crystals: A new molecular dynamics method, J. Appl. Phys. 52 (1981).
[28]A. Stukowski, Visualization and analysis of atomistic simulation data with OVITO–the Open Visualization Tool, Model. Simul. Mater. Sci. Eng. 18 (2009) 015012. doi:10.1088/0965-0393/18/1/015012.